The membrane protein Amuc_1098 from *Akkermansia muciniphila* alleviates acute pancreatitis via TLR2 signaling and glycerophospholipid metabolism remodeling

Running title: Amuc_1098 attenuates acute pancreatitis

Lijuan Wang[1,†], Ruilin Zhang[1,†], Liangtao Zhao[2,†], Liuxiang Xiao[1], Xiaoyan Zhang[1], Lingyi Liu[1], Jiaju Wang[1], Kuiyuan Chen[1], Jinyang Li[1], Maosen Zhang[3,*], Jie Li[4,*], Wei Lin[1,*]

[1] School of Medicine, Nanjing University of Chinese Medicine, Nanjing Drum Tower Hospital, Nanjing 210023, China.

[2] Hepato-Pancreato-Biliary Center, Zhongda Hospital, School of Medicine, Southeast University, Nanjing, 210009, China

[3] Jiangsu Province Hospital of Chinese Medicine, Affiliated Hospital of Nanjing University of Chinese Medicine, Nanjing, 210000, China

[4] Nanjing Drum Tower Hospital Clinical College, Nanjing University of Chinese Medicine, Nanjing, 210000, China

[*] **Corresponding author:**

Wei Lin, email: weilin@njucm.edu.cn

Jie Li, email: lijier@nju.edu.cn

Maosen Zhang, email: zms1973@yeah.net

Tel: +86-13917220653

Fax: +86-25-85811925

[†] These authors contributed equally to this work.

Supplementary Figures and Tables

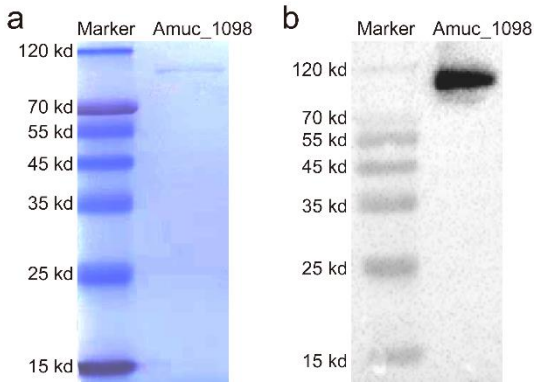

Supplementary Fig. 1: Expression and purification of Amuc_1098 *in vitro*.

a Purified Amuc_1098 was stained by Coomassie brilliant blue. **b** Purified Amuc_1098 was additionally detected by western blot.

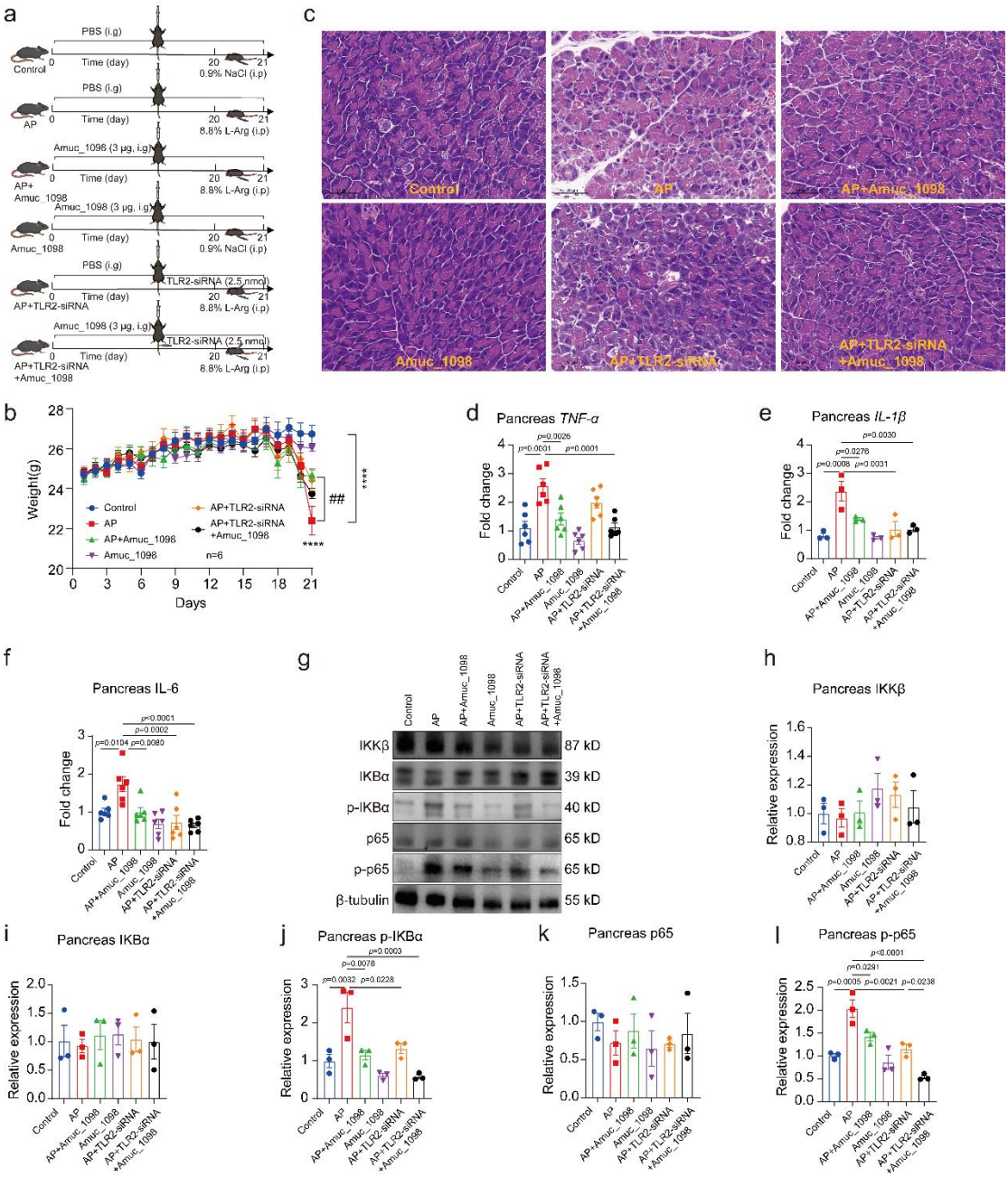

Supplementary Fig. 2: Amuc_1098 mitigates pancreatic inflammatory injury in L-Arg-induced AP mice via TLR2 mediation.

a Schematic diagram of the experimental study design. Acute pancreatitis was induced in the mice by intraperitoneal injection with 8.8% L-Arg. We administered Amuc_1098 (3 μg/mouse) in sterile phosphate buffer saline (PBS) supplemented with 2.5% glycerol to mice daily for a total of 20 days prior to L-Arg treatment. TLR2-siRNA (2.5 nM) was intraperitoneally injected into mice to construct TLR2 knockdown mice on the last day. **b** Body weight. **c** Representative histopathological sections with H&E staining of

pancreatic tissue from mice. All images were amplification 400. The mRNA expression of proinflammatory cytokines in the pancreas, including TNF-α (**d**), IL-1β (**e**), and IL-6 (**f**). **g** Western blot was used to measure NF-κB signaling pathway among three groups. The grayscale values of IKKβ (**h**), IKBα (**i**), p-IKBα (**j**), p65 (**k**), p-p65 (**l**) by Western blot. β-tubulin was used as an internal standard. Data are shown as mean ± SEM, with six biologically independent mice included in each experimental group. Significance was determined by one-way ANOVA and Tukey's multiple comparisons test.

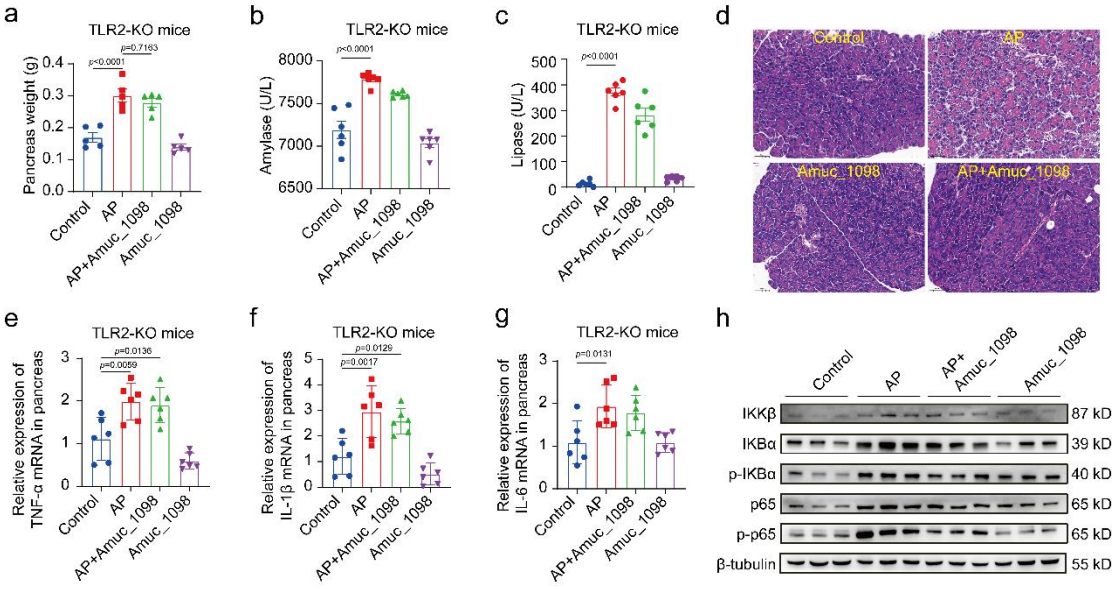

Supplementary Fig. 3: Amuc_1098-mediated protection against pancreatic injury was significantly attenuated in TLR2-deficient mice with acute pancreatitis. Following a 20-day pre-treatment with Amuc_1098 (3 μg/mouse in PBS/2.5% glycerol), acute pancreatitis was induced in TLR2-KO mice by intraperitoneal injection of caerulein (50 μg/kg, 10 hourly injections) together with LPS (5 mg/kg at the last caerulein injection). **a** Pancreas weight. Serum levels of amylase (**b**) and lipase (**c**) were measured. **d** Representative images of H&E-stained pancreatic tissue sections showing histopathological changes (original magnification, ×400). Pancreatic mRNA expression of the proinflammatory cytokines TNF-α (**e**), IL-1β (**f**), and IL-6 (**g**) was analyzed. **h** Western blot analysis was performed to assess key proteins in the NF-κB signaling pathway across the four groups, using β-tubulin as an internal control. Data are shown

as mean ± SEM, with five biologically independent mice included in each experimental group. Significance was determined by one-way ANOVA and Tukey's multiple comparisons test.

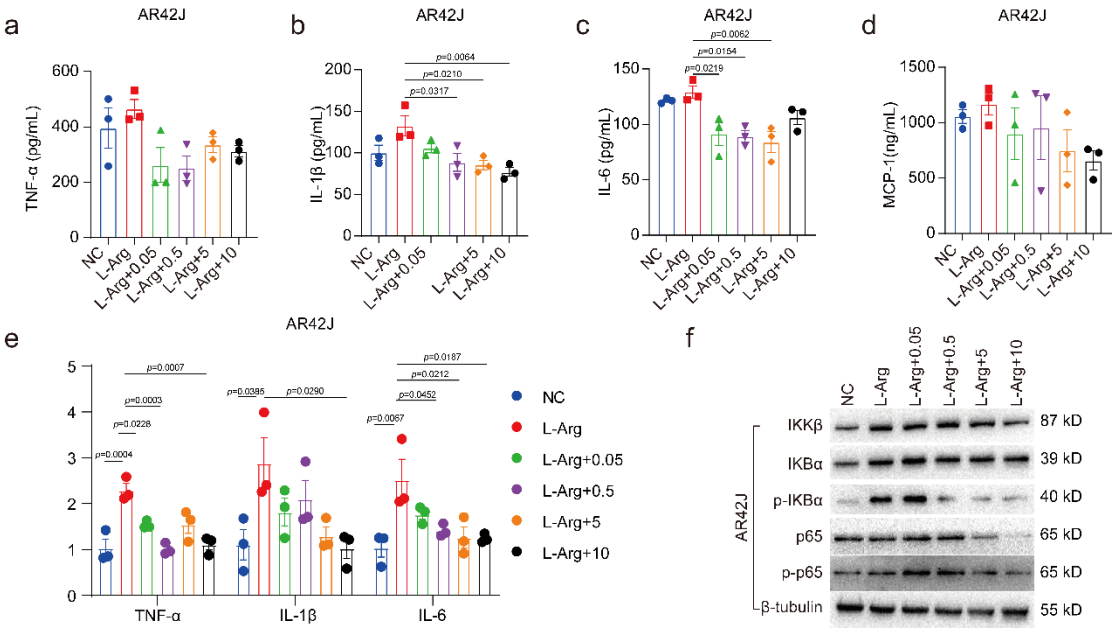

Supplementary Fig. 4: Amuc_1098* inhibited the release of inflammatory cytokines from AR42J cells *in vitro*.

To construct the AP cell model, AR42J cells were treated with 10 mg/mL L-Arg for 12 h. Then the cells were exposed to Amuc_1098* ranging from 0.05 to 10 μg/mL for 72 h. The production of TNF-α (**a**), IL-1β (**b**), IL-6 (**c**), MCP-1 (**d**) in AR42J cell culture supernatant. **e** The mRNA expression of proinflammatory cytokines in AR42J cells, including TNF-α, IL-1β, IL-6. **f** Western blot analyses of NF-κB signal pathway in AR42J cells. Data are expressed as the mean ± SEM, with each data point representing one biological replicate (n = 3 per group). Significance was analyzed using one-way ANOVA and Tukey's multiple comparisons test.

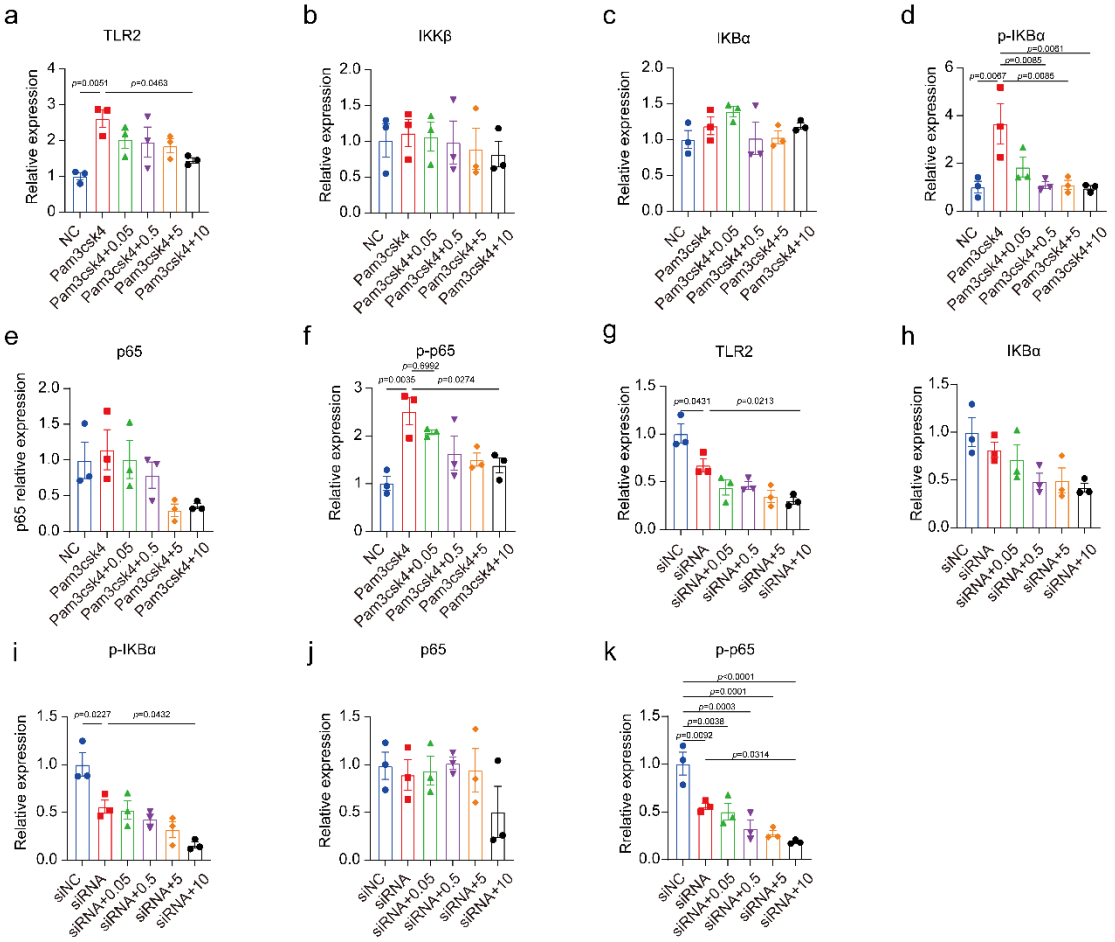

Supplementary Fig. 5: Amuc_1098 inhibited the NF-κb signaling pathway in MPC-83 cells through TLR2.

The protein levels of TLR2 (**a**), IKKβ (**b**), IKBα (**c**), p-IKBα (**d**), p65 (**e**), p-p65 (**f**) after overexpression of TLR2 in MPC-83 cells treated with different concentrations of Amuc_1098. The expression of TLR2 (**g**), IKBα (**h**), p-IKBα (**i**), p65 (**j**), p-p65 (**k**) after TLR2 knockdown in MPC-83 cells treated with different concentrations of Amuc_1098. Data are presented as the mean ± SEM (n = 3 biologically independent samples per group). Significance was analyzed using one-way ANOVA and Tukey's multiple comparisons test.

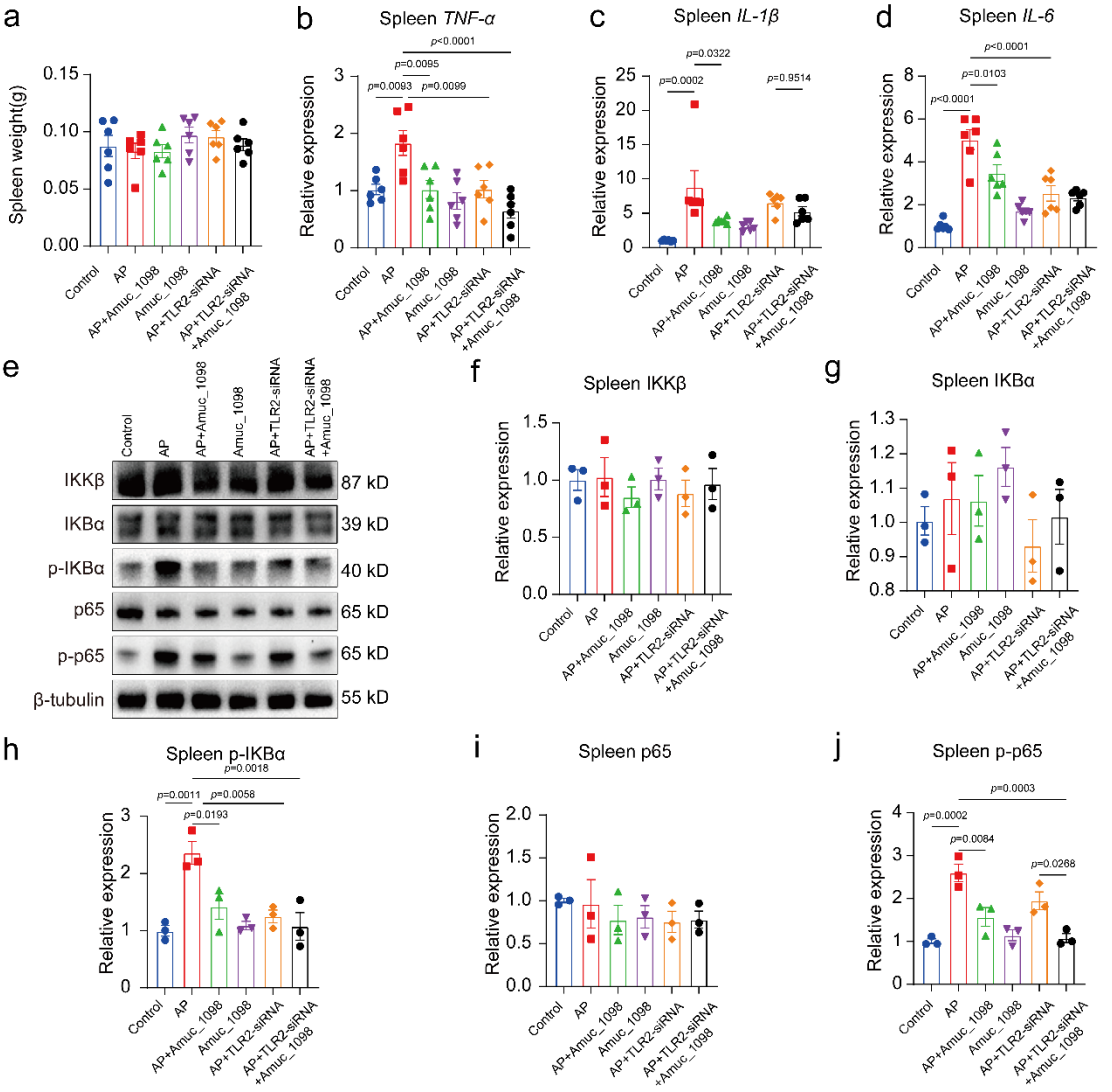

Supplementary Fig. 6: Amuc_1098 intervention in AP mice induced by L-Arg could improve Splenic inflammation.

a Spleen weight. The mRNA expression of TNF-α (**b**), IL-1β (**c**), and IL-6 (**d**) in the spleen. **e** Immunoblotting was performed to assess the expression of key NF-κB signaling components, using antibodies specific for IKKβ, IKBα, phospho-IKBα, p65, and phospho-p65. β-Tubulin was employed as an internal control. Analysis of IKKβ (**f**), IKBα (**g**), p-IKBα (**h**), p65 (**i**) and p-p65 (**j**) relative protein expression based on gray values. Data are shown as mean ± SEM, with n = 6 biologically independent mice per group. Significance was determined by one-way ANOVA and Tukey's multiple comparisons test.

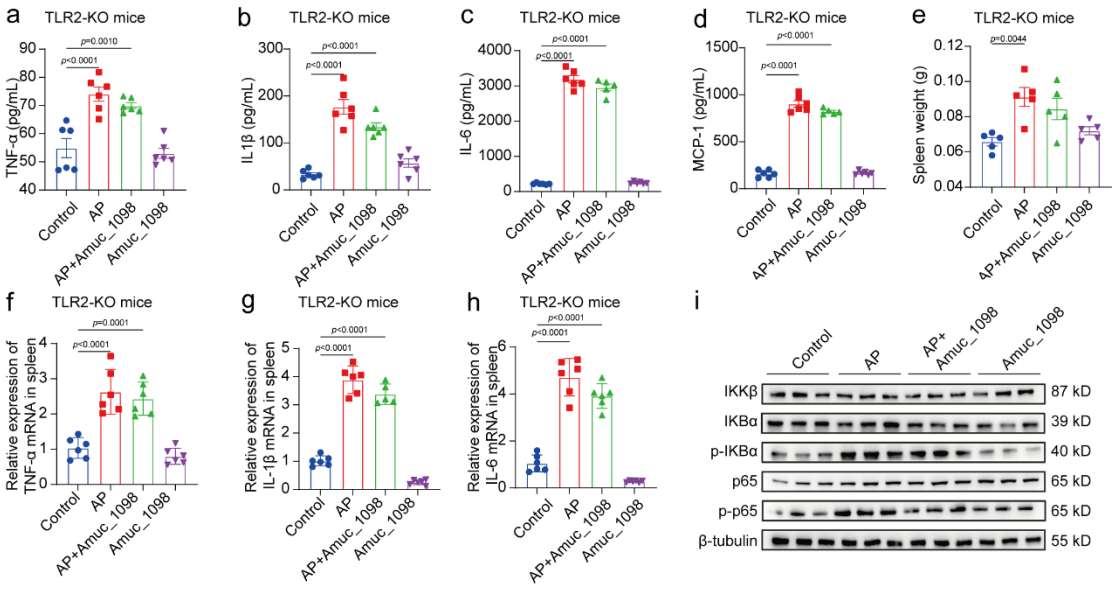

Supplementary Fig. 7: Amuc_1098 failed to alleviate splenic inflammation in TLR2-deficient mice during acute pancreatitis.

Serum levels of the inflammatory cytokines TNF-α (**a**), IL-1β (**b**), IL-6 (**c**), and MCP-1 (**d**) were measured in TLR2-knockout mice. **e** Spleen weight. The mRNA expression of TNF-α (**f**), IL-1β (**g**), and IL-6 (**h**) in the spleen. **i** Immunoblotting was performed to assess the expression of key NF-κB signaling components, using antibodies specific for IKKβ, IKBα, phospho-IKBα, p65, and phospho-p65. β-Tubulin was employed as an internal control. Data are shown as mean ± SEM, with n = 5 biologically independent mice per group. Significance was determined by one-way ANOVA and Tukey's multiple comparisons test.

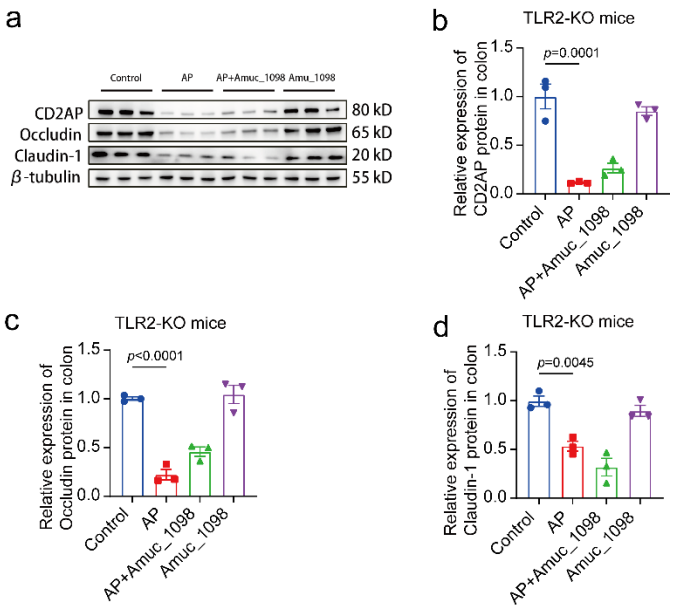

Supplementary Fig. 8: Effect of Amuc_1098 on colonic tight junction proteins in TLR2-KO mice.

a Immunoblotting was performed to detect tight junction proteins (CD2AP, Occludin, Claudin-1) in colon tissues of TLR2-KO mice, using β-tubulin as an internal control. Relative expression levels are presented for CD2AP (**b**), Occludin (**c**), and Claudin-1 (**d**). Data are shown as mean ± SEM, with n = 5 biologically independent mice per group. Significance was determined by one-way ANOVA and Tukey's multiple comparisons test.

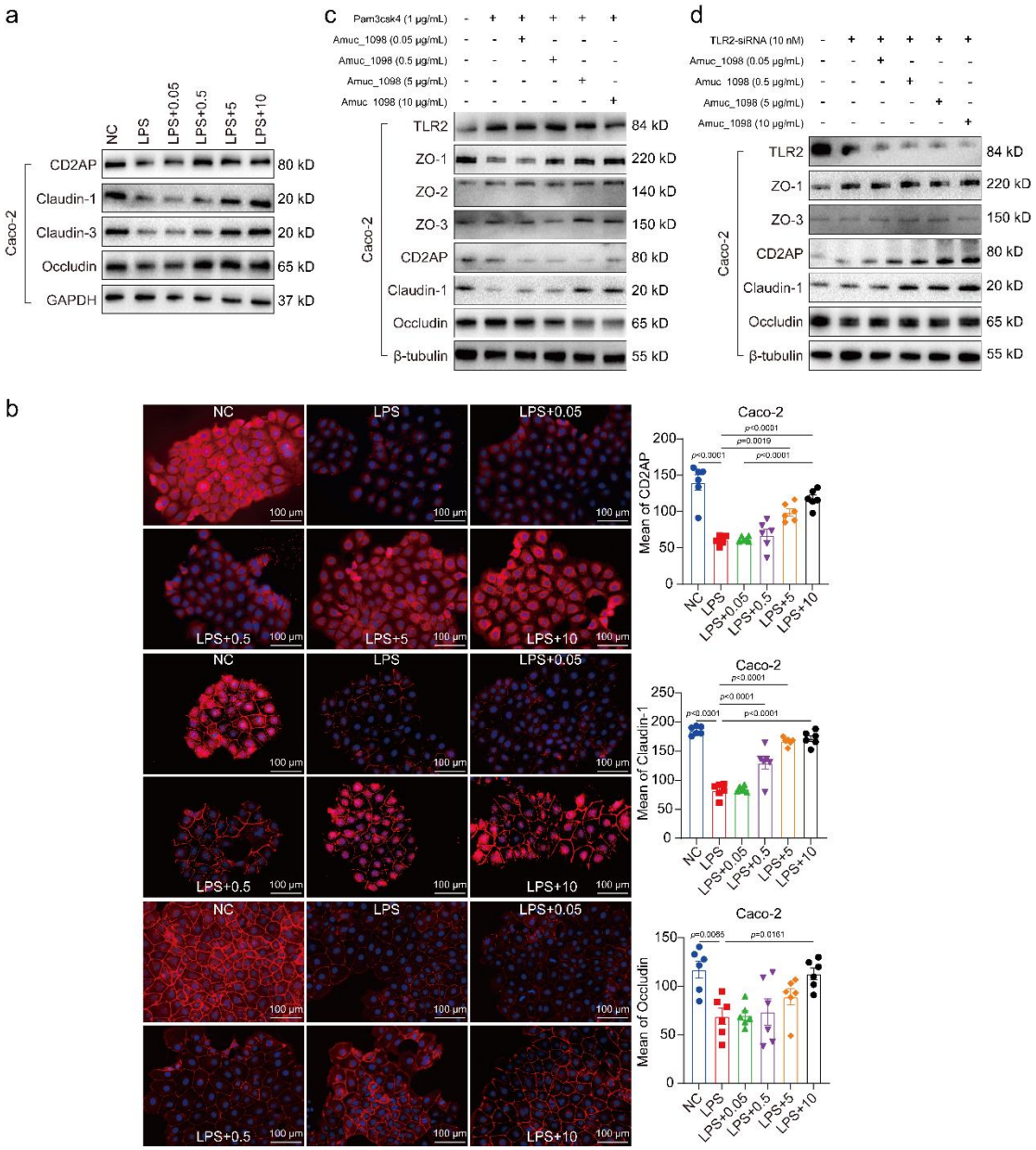

Supplementary Fig. 9: Amuc_1098 targeted TLR2 to regulated tight junction pathway in Caco-2 cells.

To establish a barrier dysfunction model, Caco-2 monolayers are treated with LPS (1 μg/mL, 24 h) and then with Amuc_1098 (0.05–10 μg/mL, 72 h). **a** The expression levels of proteins associated with the tight junction signaling pathway were assessed by western blotting. **b** Single staining of Caco-2 cells. Blue, DAP1; red, CD2AP or Claudin-1 or Occludin. Scale bars, 100 μm. **c** The level of proteins related to tight junction signaling pathway after overexpression of TLR2 in Caco-2 cells treated with different concentrations of Amuc_1098. **d** The protein expression of tight junction

signaling pathway after TLR2 knockdown in Caco-2 cells treated with different concentrations of Amuc_1098. Quantitative data are shown as mean ± SEM (n = 3 biologically independent samples per group). Immunofluorescence and immunoblot images are representative of three independent experiments. Significance was analyzed using one-way ANOVA and Tukey's multiple comparisons test.

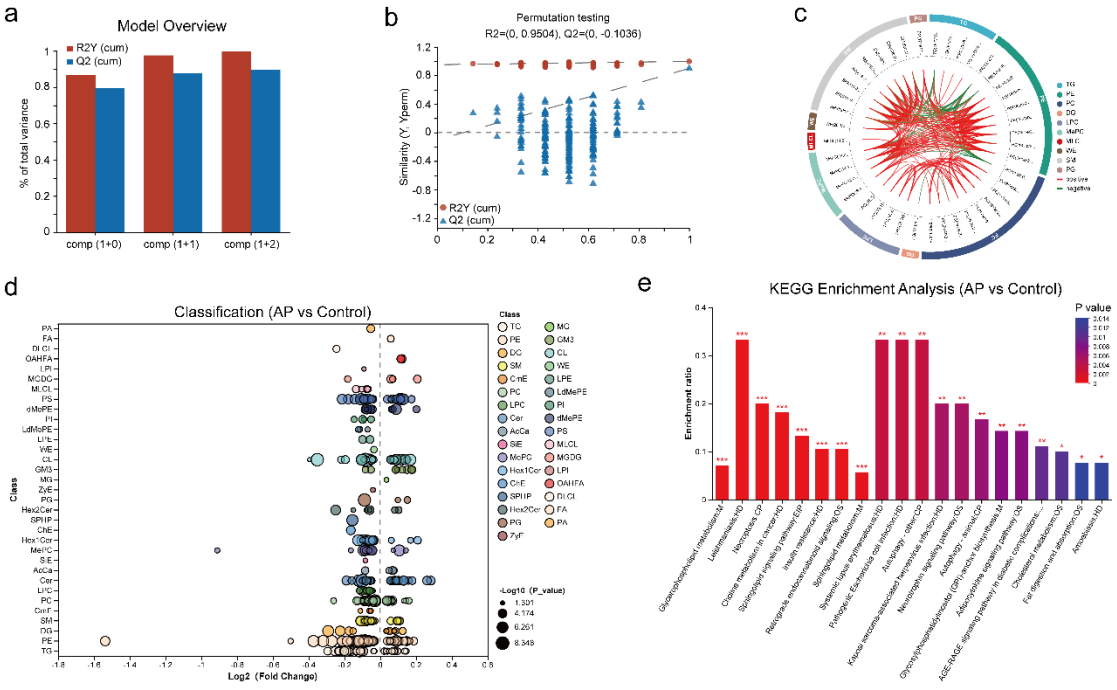

Supplementary Fig. 10: Metabolic profiling of serum from patients with AP.

a Selection of Principal Components for OPLS-DA. **b** The OPLS-DA permutation test. **c** The chord diagram, bubble chart and KEGG enrichment analysis between healthy control and AP patients. **d** The classification between AP patients and healthy control. **e** KEGG Enrichment Analysis between AP patients and healthy control. Data are presented as the mean ± SEM (n = 6 biologically independent samples per group) and were analyzed by an unpaired two-tailed Student's t-test.

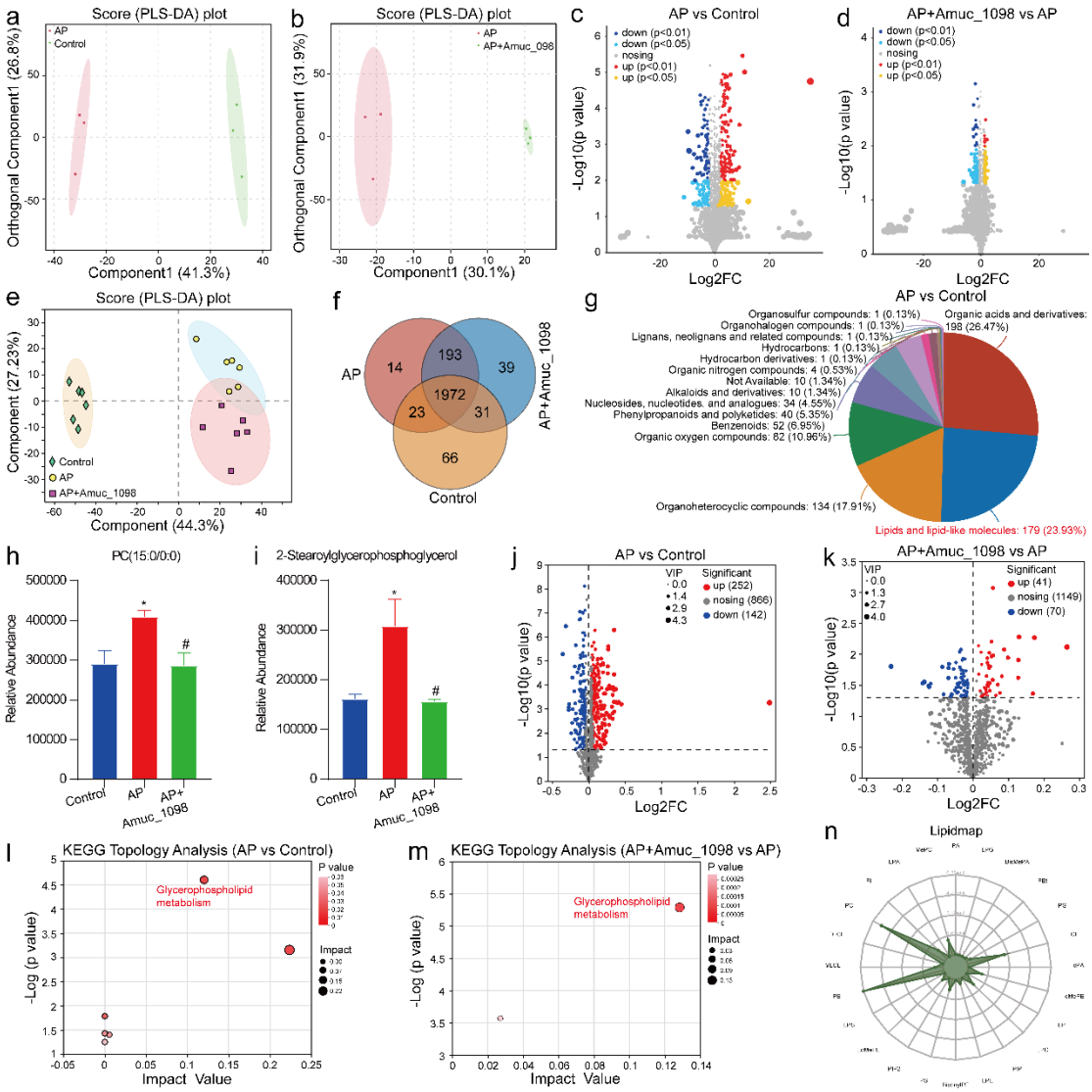

Supplementary Fig. 11: Effects of Amuc_1098 on serum metabolic profiling in mice with AP.

a-d Spatial metabolomics was used to detect pancreatic tissue metabolism in mice. PLS-DA score (**a-b**) and differential metabolite Volcano Plot (**c-d**) among control, AP and AP+Amuc_1098 groups. **e-h** Serum metabolites of mice were detected by non-target metabolomics. **e** PLS-DA score among control, AP and AP+Amuc_1098 groups. **f** Venn diagram of differential metabolites in three groups. **g** Pie chart of classification of metabolites between AP and Control. The effects of Amuc_1098 on levels of PC (15:0/0:0) (**h**) and 2-Stearoylglycerophosphoglycerol (**i**) in serum of mice. **j-n**, Lipidomics was used to detect serum lipid metabolism in mice. Differential metabolite Volcano Plot (**j-k**), KEGG topology analysis (**i-m**) and rador picture (**n**) among Control,

AP and AP+Amuc_1098 group. Data are presented as the mean ± SEM (n = 6 biologically independent samples per group) and were analyzed by one-way ANOVA followed by Tukey's multiple comparisons test.

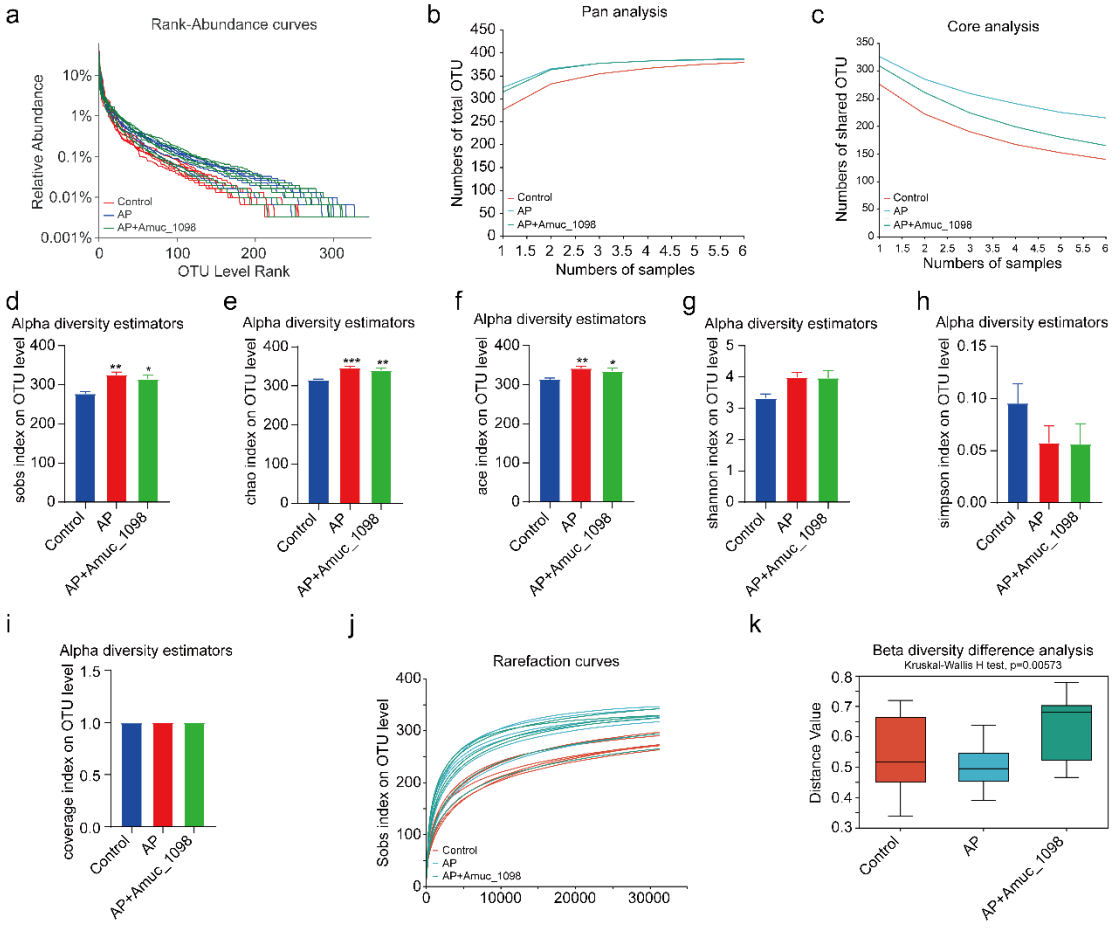

Supplementary Fig. 12: Effects of Amuc_1098 on the microbiota obtained from cecal contents in AP mice.

a OTU Rank-Abundance curves. Different samples are represented by curves of different colors. The abscissa is the number rank sorted by OTU abundance, and the ordinate is the corresponding OTU abundance. **b** Pan analysis. **c** Core analysis. Sobs (**d**), chao (**e**), ace (**f**), shannon (**g**), simpson (**h**), and coverage (**i**) index on OUT level. **j** Rarefaction curves for evaluation of microbial richness. **k** The microbiota beta diversity of group Control, AP, and AP+Amuc_1098.

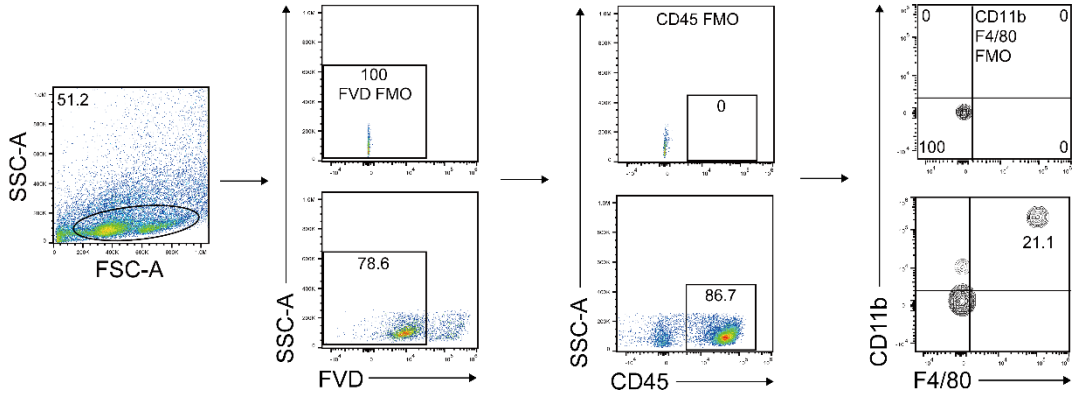

Supplementary Fig. 13: Gating strategy for flow cytometry. Cells were sequentially gated on lymphocytes (FSC/SSC), live cells (FVD), $CD45^+$ leukocytes, and finally $CD11b^+F4/80^+$ macrophages. Representative plots are shown. These gates correspond to the FACS data in Figure 4a.

Supplementary Table 1. Specific primer sequences

Gene Name	Primer sequence	
	Forward	Reverse
Mus-TNF-α	CCCTCACACTCACAAACCAC	ACAAGGTACAACCCATCGGC
Mus-IL-6	GAGGATACCACTCCCAACAGACC	AAGTGCATCATCGTTGTTCATACA
Mus-IL-1β	GCCACCTTTTGACAGTGATGAG	ATGTGCTGCTGCGAGATTTG
Mus-TLR2	ACAGCAAGGTCTTCCTGGTTCC	GCTCCCTTACAGGCTGAGTTCT
Mus-GAPDH	AGGTCGGTGTGAACGGATTTG	TGTAGACCATGTAGTTGAGGTCA
Homo-TNF-α	CTCTTCTGCCTGCTGCACTTTG	ATGGGCTACAGGCTTGTCACTC
Homo-IL-6	AGACAGCCACTCACCTCTTCAG	TTCTGCCAGTGCCTCTTTGCTG
Homo-IL-1β	CCACAGACCTTCCAGGAGAATG	GTGCAGTTCAGTGATCGTACAGG
Homo-TLR-2	CTTCACTCAGGAGCAGCAAGCA	ACACCAGTGCTGTCCTGTGACA
Homo-GAPDH	GTCTCCTCTGACTTCAACAGCG	ACCACCCTGTTGCTGTAGCCAA
Rat-TNF-α	TGAAATGCCACCTTTTGACAGTGAT	GCCTGCCTGAAGCTCTTGTTG
Rat-IL-6	TAGTCCTTCCTACCCCAATTTCC	TTGGTCCTTAGCCACTCCTTC
Rat-IL-1β	TGAAATGCCACCTTTTGACAGTGAT	GCCTGCCTGAAGCTCTTGTTG
Rat-TLR2	GATCCAGAGCAACACTCTCAACAT	CTCCAGACCATGAAGTTGACAAAC
Rat-GAPDH	TGGAGTCTACTGGCGTCTT	TGTCATATTTCTCGTGGTTCA

Supplementary Table 2. Antibodies

Antibodies	Use	Source	Identifier
β-tubulin Antibody	Western Blot	Cell Signaling Technology	#2146
NF-κB p65 (D14E12) XP® Rabbit mAb	Western Blot	Cell Signaling Technology	#8242
Phospho-NF-κB p65 (Ser536) (93H1) Rabbit mAb	Western Blot	Cell Signaling Technology	#3033
IKKα (3G12) Mouse mAb	Western Blot	Cell Signaling Technology	#11930
IKKβ (D30C6) Rabbit mAb	Western Blot	Cell Signaling Technology	#8943
IκBα (L35A5) Mouse mAb (Amino-terminal Antigen)	Western Blot	Cell Signaling Technology	#4814
Phospho-IκBα (Ser32) (14D4) Rabbit mAb	Western Blot	Cell Signaling Technology	#2859
GAPDH (14C10) Rabbit mAb	Western Blot	Cell Signaling Technology	#2118
CD2AP Antibody	Western Blot	Cell Signaling Technology	#2135
Claudin-1 (D5H1D) XP® Rabbit mAb	Western Blot	Cell Signaling Technology	#13255
Claudin-3 (D7A3O) Rabbit mAb	Western Blot	Cell Signaling Technology	# 83609
Occludin (E6B4R) Rabbit mAb	Western Blot	Cell Signaling Technology	# 91131
ZO-1 (D7D12) Rabbit mAb	Western Blot	Cell Signaling Technology	#8193
ZO-2 Antibody	Western Blot	Cell Signaling Technology	#2847
ZO-3 (D57G7) XP® Rabbit mAb	Western Blot	Cell Signaling Technology	#3704
Toll-like Receptor 2 (D7G9Z) Rabbit Monoclonal Antibody	Western Blot	Cell Signaling Technology	#12276
Toll-like Receptor 2 (E1J2W) Rabbit Monoclonal Antibody	Western Blot	Cell Signaling Technology	#13744